



Investigating the yield of H₂O and H₂ from methane oxidation in the stratosphere

Franziska Frank¹, Patrick Jöckel¹, Sergey Gromov^{2,3}, and Martin Dameris¹

¹Deutsches Zentrum für Luft- und Raumfahrt (DLR), Institut für Physik der Atmosphäre, Oberpfaffenhofen, Germany

²Max-Planck-Institute for Chemistry, Air Chemistry Department, Mainz, Germany

³Institute of Global Climate and Ecology Roshydromet & RAS (IGCE), Moscow, Russia

Correspondence: Franziska Frank (franziska.frank@dlr.de)

Received: 14 February 2018 – Discussion started: 5 March 2018

Revised: 2 July 2018 – Accepted: 3 July 2018 – Published: 13 July 2018

Abstract. An important driver of climate change is stratospheric water vapor (SWV), which in turn is influenced by the oxidation of atmospheric methane (CH₄). In order to parameterize the production of water vapor (H₂O) from CH₄ oxidation, it is often assumed that the oxidation of one CH₄ molecule yields exactly two molecules of H₂O. However, this assumption is based on an early study, which also gives evidence that this is not true at all altitudes.

In the current study, we re-evaluate this assumption with a comprehensive systematic analysis using a state-of-the-art chemistry–climate model (CCM), namely the ECHAM/MESy Atmospheric Chemistry (EMAC) model, and present three approaches to investigate the yield of H₂O and hydrogen gas (H₂) from CH₄ oxidation. We thereby make use of the Module Efficiently Calculating the Chemistry of the Atmosphere (MECCA) in a box model and global model configuration. Furthermore, we use the kinetic chemistry tagging technique (MECCA-TAG) to investigate the chemical pathways between CH₄, H₂O and H₂, by being able to distinguish hydrogen atoms produced by CH₄ from H₂ from other sources.

We apply three approaches, which all agree that assuming a yield of 2 overestimates the production of H₂O in the lower stratosphere (calculated as 1.5–1.7). Additionally, transport and subsequent photochemical processing of longer-lived intermediates (mostly H₂) raise the local yield values in the upper stratosphere and lower mesosphere above 2 (maximum > 2.2). In the middle and upper mesosphere, the influence of loss and recycling of H₂O increases, making it a crucial factor in the parameterization of the yield of H₂O from CH₄ oxidation. An additional sensitivity study with the

Chemistry As A Boxmodel Application (CAABA) shows a dependence of the yield on the hydroxyl radical (OH) abundance. No significant temperature dependence is found. We focus representatively on the tropical zone between 23° S and 23° N. It is found in the global approach that presented results are mostly valid for midlatitudes as well. During the polar night, the method is not applicable.

Our conclusions question the use of a constant yield of H₂O from CH₄ oxidation in climate modeling and encourage to apply comprehensive parameterizations that follow the vertical profiles of the H₂O yield derived here and take the chemical H₂O loss into account.

1 Introduction

It is beyond question that water vapor (H₂O) is an important greenhouse gas (GHG). The current study focuses on stratospheric water vapor (SWV), which is by itself an influential driver of climate change. SWV, for example, induces a reduction of stratospheric ozone concentration (Stenke and Grewe, 2005; Revell et al., 2016), cools the stratosphere (Revell et al., 2012; Forster and Shine, 1999; Maycock et al., 2014) and produces a positive radiative forcing (Solomon et al., 2010). Changes in SWV are mainly driven by troposphere–stratosphere exchange (e.g., through deep convection in the tropics; Fueglistaler and Haynes, 2005). However, there is also a chemical contribution to SWV, mostly by oxidation of methane (CH₄) and hydrogen gas (H₂). These gases are still abundant above the tropopause to act as significant in situ photochemical sources of H₂O. Besides H₂O, CH₄ is a

powerful GHG as well, with a 34 times higher climate effect than an equivalent amount of carbon dioxide (CO₂) on a time horizon of 100 years (IPCC, 2013). It also introduces secondary climate effects through the additional SWV. The strong linkage of CH₄ and SWV represents a decisive factor of the net climate effect of CH₄. Enhanced CH₄ concentrations are likely expected in the future Earth's atmosphere and can impact the otherwise rather dry stratosphere substantially (Rohs et al., 2006).

Nevertheless, to account for the contribution of CH₄ to SWV, in current climate modeling it is common either to use a chemistry–climate model (CCM) with a complex chemistry setup, which puts high demands on computational resources, or a general circulation model (GCM) or chemical transport model (CTM) with – if at all – a parameterization of the chemical sources of SWV. A parameterization of the chemical feedback onto SWV requires to estimate the yield of H₂O from CH₄ oxidation, which is defined as the production of H₂O per oxidized CH₄ molecule. A common simple assumption of the yield of H₂O from CH₄ oxidation is that one oxidized CH₄ molecule produces two H₂O molecules in the stratosphere. This simple parameterization is based on a first estimation of the H₂O yield from CH₄ oxidation, using a simplified methane chemistry without chlorine in a two-dimensional photochemistry model (le Texier et al., 1988).

This is a widely accepted approximation (Myhre et al., 2007; Stowasser et al., 1999) and is also affirmed by aircraft observations, which state that $2 \cdot [\text{CH}_4] + [\text{H}_2\text{O}]$ (also named as the total stratospheric hydrogen budget) is fairly constant in the stratosphere being 6.8–7.6 ppmv (Hurst et al., 1999; Rahn et al., 2003; Dessler et al., 1994; Stowasser et al., 1999). Although this suggests that all atomic hydrogen (H) from CH₄ oxidation reaches H₂O, it must be noted that the referenced observation studies do not distinguish whether the H in H₂O comes from CH₄ or from H₂, which also originates from the troposphere. Thus, calculations based on observed mixing ratios show a net production of H₂O only but not the yield of H₂O specifically from CH₄ oxidation (Hurst et al., 1999). Furthermore, H₂ mixing ratios, when measured as well, show an almost absent vertical gradient, which can be explained by the supposition that the H₂ sink is in photochemical equilibrium with its production from CH₄ oxidation. Hence, all additional H₂ by CH₄ is leveled by the oxidation of H₂ and balances the $2 \cdot [\text{CH}_4] + [\text{H}_2\text{O}]$ and H₂ content in the stratosphere (Rahn et al., 2003). Nevertheless, Hurst et al. (1999) took the weak anticorrelation of H₂ and CH₄ into account and calculated a net production of H₂O over loss of CH₄ of 1.973 ± 0.003 , differing from the assumed value of 2, which would be the case if all H went into H₂O. By analyzing satellite-based measurements, Wrotny et al. (2010) derived a production of H₂O over loss of CH₄ ratio of 2.0–3.7 in the upper stratosphere between 1.0 and 4.6 hPa, which is clearly ≥ 2 .

Still, for reasons of simplification, several GCMs use the approximation that the yield of H₂O from CH₄ oxidation is

exactly 2 (Monge-Sanz et al., 2013; ECMWF, 2007; Austin et al., 2007; Oman et al., 2008; Boville et al., 2001; Mote, 1995; Eichinger et al., 2015). In the ECHAM/MESSy Atmospheric Chemistry (EMAC) model (Jöckel et al., 2010), for example, explicitly configured in a CTM-like setup without interactive chemistry, the production of SWV from CH₄ oxidation is calculated in a simplified way using a specifically introduced CH₄ tracer (by applying the CH₄ submodel) according to

$$\frac{d}{dt}[\text{H}_2\text{O}] = -\gamma_{\text{H}_2\text{O}} \cdot \frac{d}{dt}[\text{CH}_4], \quad (1)$$

with $\gamma_{\text{H}_2\text{O}} = 2$ as the yield of H₂O. Note that, if one wants to apply such a parameterization, one must specifically be careful not to mix the yield of H₂O from the oxidation of CH₄ ($\gamma_{\text{H}_2\text{O}}$) with the yield from the oxidation of H₂, originating from the troposphere.

However, this approximation first and foremost neglects the chemical loss of H₂O (mostly by reaction with excited oxygen, O(¹D), and by photolysis). Using this parameterization, SWV is solely added and not removed by chemistry. Moreover, the results of le Texier et al. (1988) also suggest that the yield of H₂O from CH₄ oxidation is not exactly 2, accounting for the part of H diverted into H₂ production, and that the share of H₂ increases at higher altitudes. Therefore, following the results of le Texier et al. (1988) precisely, we would generate a certain bias by using a yield of 2 in Eq. (1), especially at higher altitudes, where $2 \cdot [\text{CH}_4] + [\text{H}_2\text{O}]$ approximately constant does not hold anymore. In the mesosphere, for example, the loss of H₂O becomes increasingly relevant, shifting the balance between H₂O and H₂ towards the latter. Furthermore, the net production calculated by Hurst et al. (1999) and the yield of le Texier et al. (1988) also do not agree well in the lower stratosphere, which can indeed be explained by the indistinguishable inputs from H₂ and CH₄ oxidation in observations as stated before. Yet, this does also indicate that the yield from CH₄ oxidation itself must be even lower than suggested by the net production, which is calculated based on observations. It is, therefore, questionable if the assumption of $\gamma_{\text{H}_2\text{O}} = 2$ for the CH₄ oxidation is indeed applicable.

In this study, we re-evaluate the findings of le Texier et al. (1988) with multiple approaches using a modern CCM with a complex state-of-the-art chemistry mechanism. Our goal is to assess the currently used assumption of the constant yield as in Eq. (1) with $\gamma_{\text{H}_2\text{O}} = 2$ and investigate if a parameterization solely based on CH₄ is sufficient to reproduce the chemical yield of H₂O from CH₄ oxidation. As an additional remark, it should be noted that difficulties with yield estimates can be expected especially in the stratosphere, as it is vertically not as well mixed as the turbulent troposphere.

We show three approaches to determine the yield of H₂O from CH₄ oxidation. The first two approaches use the kinetic chemistry tagging technique (MECCA-TAG; Gromov et al., 2010), either (1) in a box model setup with the Chemistry As A Boxmodel Application (CAABA; R. Sander et al., 2011) and (2) in a global simulation, with the EMAC (Jöckel et al., 2010) model. For the third approach (3), we again use the model results of a global simulation with EMAC. This approach relies on the assumption that the hydrogen budget in the stratosphere is conserved, mostly consisting of fractions of H, H₂, H₂O and CH₄.

We apply MECCA-TAG (Gromov et al., 2010) in all approaches to run a comprehensive chemistry setup, while being able to track the production of H₂O originating explicitly from CH₄ oxidation. A conceptually different approach would be the extended Crutzen sequential method used by Johnston and Kinnison (1998) to estimate the gross ozone loss by CH₄. The study of Johnston and Kinnison (1998) is an additional example for estimating a yield from CH₄ oxidation, although it focuses on CH₄ impacts on ozone (O₃) instead of H₂O. By applying MECCA-TAG, however, it is not necessary to explicitly write down the chemical net reactions as this is done in the extended Crutzen sequential method.

The paper is structured as follows. In Sect. 2, we present the methods and theoretical background of our studies, followed by the results in Sect. 3. Section 4 comprises a detailed discussion and Sect. 5 summarizes the findings and gives an outlook for further studies.

2 Methods

2.1 The model setup

2.1.1 EMAC

The applied global chemistry climate model is EMAC, which is a state-of-the-art numerical chemistry and climate simulation system that includes submodels describing tropospheric and middle atmosphere processes and their interaction with oceans, land and human influences (Jöckel et al., 2010). It uses the second version of the Modular Earth Submodel System (MESSy) to link multi-institutional computer codes. The core atmospheric model is the European Centre Hamburg general circulation model (ECHAM5) (Roeckner et al., 2006). For the global simulations, in the present study, we applied EMAC (ECHAM5 version 5.3.02, MESSy version 2.53.0) in the T42L90MA resolution, i.e., with a spherical truncation of T42 (corresponding to a quadratic Gaussian grid of approximately 2.8° by 2.8° in latitude and longitude) with 90 vertical hybrid pressure levels up to 0.01 hPa. The applied model setup comprises particularly the submodels Module Efficiently Calculating the Chemistry of the Atmosphere (MECCA) (Sander et al., 2005) and MECCA-TAG (Gromov et al., 2010).

The submodel MECCA represents the chemical core of EMAC. The applied chemistry is based on a chemical mechanism, which, for example, was already used for the base simulations in the Earth System Chemistry integrated Modelling (ESCiMo) project (Jöckel et al., 2016). The mechanism is extended to resolve specific intermediates in the CH₄ → H₂O reaction chain (e.g., methyl (CH₃) and methoxy radical (CH₃O), resulting in slightly more comprehensive chemical kinetics. The full chemical mechanism is part of the Supplement.

2.1.2 The kinetic tagging technique MECCA-TAG

MECCA-TAG (Gromov et al., 2010) enables the user to tag certain elements without modifying the underlying standard chemical mechanism. It can either be applied for simulating isotopologues of selected trace gases or used to investigate elemental exchange between the species of interest. For example, a model study was carried out with focus on the carbon and oxygen isotope composition of carbon monoxide (CO) (Gromov et al., 2010).

In the current study, we use the tagging technique (in the so-called fractional mode) to investigate the pathways of H atom transfer from the source CH₄ to H₂O via all simulated intermediates. In order to do so, we create counterparts of the species of interest (e.g., those containing H) in an isolated doubled set of studied reactions (e.g., CH₄ oxidation chemistry) in the same chemical mechanism simulated. By doing so, we are able to quantify the fraction of molecules (hence their H content) stemming from CH₄ oxidation only, as well as their production and loss rates, which are used for the yield calculations. Furthermore, we improve the latter by quantifying the H, which is recycled in the given reactions.

In this particular case, we count the H₂O molecules created from CH₄ oxidation pathways and are able to distinguish the H from CH₄ from the H of other sources (H₂, non-methane hydrocarbons (NMHCs), hydrochlorofluorocarbons (HCFCs), etc.). More specifically, we track the H atoms, which all have in common that their source is only CH₄. These H atoms can temporarily be part of H₂, but we are not counting oxidation of H₂, which is produced in the troposphere and transported into the stratosphere. However, we are accounting for hydrogen, which has been part of CH₄ produced H₂O, and which becomes recycled after depletion of H₂O. Hence, that part of CH₄-produced H₂O, which breaks down to other HO_x (hydroxyl radical, OH, and hydroperoxyl radical, HO₂) compounds (and subsequently produces H₂O again), is counted separately. Overall, such an approach is the “online” approximation of the technique used by Lehmann (2004) and helps to avoid double-counting issues in yield derivation. Ultimately, we are able to quantify the fraction of H atoms populating the species of the complete (CH₄ → H₂O / H₂ ↔ HO_x) cycle, including their fractions recycled via H₂O.

2.1.3 CAABA

For the photochemical box model studies, we use CAABA in model version 3.0 (R. Sander et al., 2011). CAABA equipped with MECCA (CAABA/MECCA) provides an atmospheric chemistry box model, simulating single air parcels with the chemical mechanism identical to that used in EMAC. CAABA/MECCA is, moreover, using the MESSy interface to attach certain submodels to the box model system. The used submodels in the current study, in addition to MECCA, are SEMIDEP (which applies deposition fluxes) and JVAL (which calculates photolysis rates) (Sander et al., 2014).

CAABA simulates one box at one pressure and temperature specific for a given latitude and altitude in the atmosphere. To derive a pseudo-vertical profile of the yield, 35 independent boxes superimposed upon each other at the Equator are simulated with prescribed conditions following a standard atmosphere profile (NOAA/NASA, 1976; accessed via <https://www.digitaldutch.com/atmoscalc/>; digital dutch, 1999). The equatorial region is chosen for mainly two reasons: (1) the equatorial region is in terms of photochemistry most active, and (2) we avoid the inactive photochemistry during the polar night. Since the boxes represent different temperature and pressure levels and therefore distinct chemical regimes throughout the middle atmosphere, it is possible to illustrate the vertical dependence of the yield.

Note that the purpose of the box model simulation is to demonstrate the steady state conditions expected at different altitudes. In order to do so, we mimic the effect of vertical transport between the boxes by prescribing the vertical distribution of the relevant species concentrations for

1. CH₄ and all species acting as in situ sources of H (primarily NMHCs and HCFCs), which are not produced in the chemical mechanism;
2. long-lived substances, such as ammonia (NH₃) and nitrous oxide (N₂O);
3. N₂ and O₂, whose mixing ratios are virtually constant throughout the considered altitude range;
4. nitrogen oxide (NO) and O(¹D), to constrain the HO_x–NO_x cycle to the given initial state (the NO_x family consists of NO and nitrogen dioxide, NO₂);
5. SO₂, chlorine (Cl) and Br, for the same reason as in 4 with respect to ClO_x (Cl + ClO), BrO_x (Br + BrO) and sulfate compounds; and
6. H₂O and H₂ mixing ratios and therefore serving as a H sink for the limitless influx of H via the fixed source species (indicated in 1).

Other species, particularly the OH and HO₂, are unconstrained in the simulations unless otherwise noted. All initial mixing ratios of the chemical species are taken from a

climatology over the years 2000–2010 of the RC1SD-base-07 EMAC simulation of the ESCiMo project (Jöckel et al., 2016). This simulation is carried out at T42L90MA resolution with specified dynamics; hence, a Newtonian relaxation is performed with respect to meteorological reference data (ERA-Interim reanalysis data from ECMWF (Dee et al., 2011) to be more precise) concerning the prognostic variables divergence, vorticity, temperature and (logarithm of) surface pressure.

Because a priori fractions of H from CH₄ (or tagged H) in the species of the chemical mechanism are not known, all tagged species are initialized with zero. The simulation of every box is run for 200 years to make sure that all tagged species have filled up to a steady state.

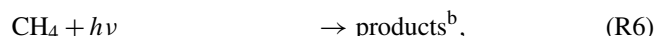
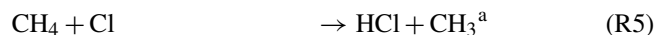
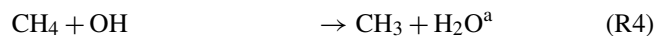
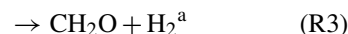
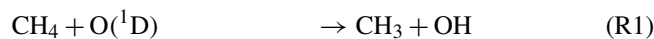
2.2 Calculation of the chemical H₂O yield from CH₄ oxidation

A straightforward definition of the direct yield is the ratio of the production of H₂O molecules to the loss of CH₄, as depicted in Eq. (2).

$$\gamma_{\text{H}_2\text{O}}^{\text{direct}}(\text{CH}_4) = \frac{\mathbf{P}_{\text{H}_2\text{O}}^{\text{I}}}{\mathbf{L}_{\text{CH}_4}}, \quad (2)$$

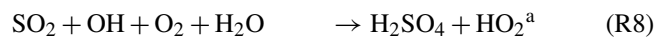
with variables listed in Table 1. The yield $\gamma_{\text{H}_2\text{O}}$ represents the units of molecule H₂O per molecule CH₄, i.e., (molecule molecule⁻¹), and is displayed dimensionless throughout this work.

The loss of CH₄ (\mathbf{L}_{CH_4}) in MECCA includes the reactions with OH, O(¹D) and Cl, as well as photolysis (see Reactions R1–R6).



with reaction rates of a from S. P. Sander et al. (2011) and photolysis rate of b calculated by JVAL (Sander et al., 2014).

Following these reactions, H atoms from CH₄ are distributed among intermediates (not shown) and eventually reach H₂O. Produced H₂O reacts further and gets removed by Reactions (R7) and (R9).

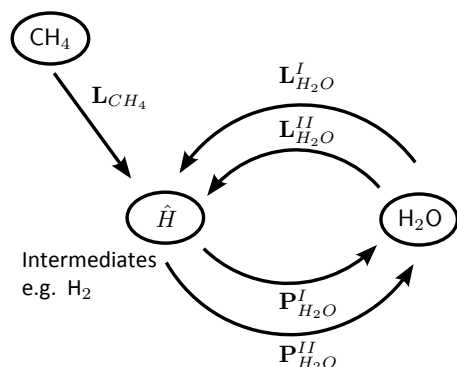


with reaction rates of a from S. P. Sander et al. (2011) and photolysis rate of b calculated by JVAL (Sander et al., 2014).

In consecutive reactions, H is again recycled into H₂O. The direct yield calculated by Eq. (2) represents the H₂O,

Table 1. Variable names as used in Eqs. (2), (3) and (4).

Name	Description
L_{CH_4}	Loss of CH ₄ molecules
$P_{\text{H}_2\text{O}/\text{H}_2}^{\text{I}}$	Direct production of H ₂ O/H ₂ by H from CH ₄
$L_{\text{H}_2\text{O}/\text{H}_2}^{\text{I}}$	Loss of directly produced H ₂ O/H ₂
$P_{\text{H}_2\text{O}/\text{H}_2}^{\text{II}}$	Production of recycled H ₂ O/H ₂ , Hence, the H already has been part Of a H ₂ O/H ₂ produced by CH ₄
$L_{\text{H}_2\text{O}/\text{H}_2}^{\text{II}}$	Loss of recycled H ₂ O/H ₂
$\mu_{\text{H}_2\text{O}/\text{H}_2}$	Lost H ₂ O/H ₂ during the recycling

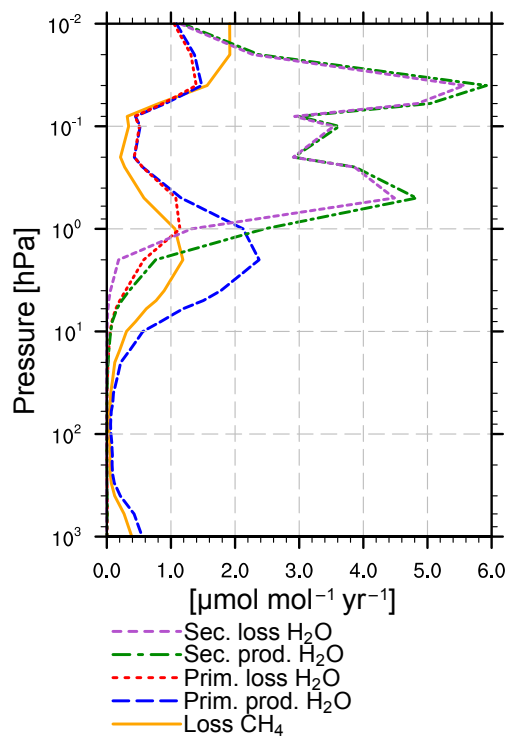
**Figure 1.** Sketch on the production and recycling of H₂O. The arrows of L_{CH_4} and $P_{\text{H}_2\text{O}}^{\text{I}}$ indicate the direct yield, and all arrows together indicate the effective yield.

which is produced in the chemical mechanism and directly emerges from CH₄ oxidation. However, this is not the additional H₂O of the whole chemical process. It also cannot be used in a simplified setup for the methane chemistry and the production of SWV parameterized as by Eq. (1), because no chemical depletion of water is considered. Hence, we suggest to define the effective yield of H₂O, which takes into account that water is recycled in consecutive reactions and that recycled water is again destroyed. The process is sketched in Fig. 1. During this recycling process, some H is converted to species other than H₂O, filling up to a steady state or leaving the HO_x cycle once and for all. The effective yield is therefore always equal to or smaller than the direct yield in a closed system.

We define the effective yield of H₂O in this study as in Eq. (3), with μ accounting for the lost H₂O, due to subsequent loss and recycling of H₂O molecules:

$$\gamma_{\text{H}_2\text{O}}^{\text{eff}}(\text{CH}_4) = \frac{P_{\text{H}_2\text{O}}^{\text{I}} - \mu_{\text{H}_2\text{O}}}{L_{\text{CH}_4}} \quad \text{with} \quad \mu_{\text{H}_2\text{O}} = L_{\text{H}_2\text{O}}^{\text{I}} + L_{\text{H}_2\text{O}}^{\text{II}} - P_{\text{H}_2\text{O}}^{\text{II}}. \quad (3)$$

Variables are listed in Table 1.

**Figure 2.** Separate loss of CH₄, and primary and secondary loss and production of H₂O from box model simulation Ref.

Exemplarily, the components of the effective yield of H₂O of Eq. (3) are plotted separately in Fig. 2 as a vertical profile for the experiment Ref, which will be introduced in more detail in Sect. 3.1.2. These profiles indicate that loss of CH₄ and production of H₂O minimize around the tropopause and maximize close to the stratopause. The maximum of the primary loss of H₂O in the stratosphere is slightly shifted vertically. Above the stratopause, the recycling of H₂O becomes more important. This is indicated by increased secondary loss and production of H₂O and is further reflected by the reduced effective yield in the mesosphere.

Due to the implementation of the tagging technique, counting of recycled H (as described in Sect. 2.1.2) can only be applied with respect to one species at a time. Hence, the effective yield can only be calculated either for H₂O or H₂ in the same simulation. Similar to that for H₂O, recycling of H₂ is calculated in the chemical mechanism; that is, the recycled H is counted as soon as it is leaving H₂. The corresponding formula for H₂ is derived similarly to Eq. (3) and reads as follows:

$$\gamma_{\text{H}_2}^{\text{eff}}(\text{CH}_4) = \frac{P_{\text{H}_2}^{\text{I}} - \mu_{\text{H}_2}}{L_{\text{CH}_4}} \quad \text{with} \quad \mu_{\text{H}_2} = L_{\text{H}_2}^{\text{I}} + L_{\text{H}_2}^{\text{II}} - P_{\text{H}_2}^{\text{II}}. \quad (4)$$

Direct and effective yield are equal, as long as the loss of H₂O is negligible or the recycling is lossless.

The chemical conversion from CH₄ to H₂O follows some intermediate reactions. Hence, the loss of CH₄ and the even-

tual production of H₂O do not occur simultaneously. Furthermore, in reality, chemistry undergoes diurnal variations. The major changes occur during daylight. At night, virtually no photosensitive chemistry takes place, which results in very low OH concentrations. This reduces CH₄ loss and H₂O production to a nighttime low. A diurnal average smoothes the difference between day and night to a representative value. This is based on the assumption that the system is in a quasi-steady state. A quasi-steady state implies that equal integral production and loss are simulated throughout a given time interval, e.g., a day, a month or a year. Monthly $\gamma_{\text{H}_2\text{O}}$ averages, as presented in this study, which average over the simulated diurnal cycle, are sufficient for the application of a simplified CH₄ loss / H₂O production rate calculation with prescribed monthly varying OH distributions.

For these reasons, we apply Eq. (3) in our analysis to annual averages of the production and sink terms simulated in the boxes representing conditions typical for the tropics, where in addition seasonal variations are negligible. In the global simulations with EMAC, we calculate an average over zonally averaged tropical bands.

In the following, we compare the direct and effective yields of H₂O and H₂ from CH₄ oxidation obtained in simulations with the box model and EMAC.

3 Results

3.1 Box model approach

3.1.1 Simulation with unrestrained oxidation capacity

The direct and the effective yields of H₂O from CH₄ oxidation of the box model approach (i.e., simulation Exp1), calculated as indicated in Eqs. (2) and (3), respectively, are shown as a pseudo-vertical profile in Fig. 3 by 35 vertically stacked boxes following the standard atmosphere at the Equator. The shown results comprise also boxes on tropospheric levels. However, since the physical water cycle (e.g., evaporation, clouds) exceeds the influence of the CH₄ oxidation on H₂O, the kinetic production of H₂O is irrelevant in the troposphere. All values below the tropopause level (approximately 100 hPa in the tropics) are therefore not part of the analysis presented in this work.

The direct yield in Fig. 3a is 1.7 around the tropopause and increases monotonically up to 2 at 4 hPa. It remains constant until 0.2 hPa, where it starts to decrease monotonically down to about 0.65 at the uppermost layer. In the mesosphere, the loss of H₂O especially via Reactions (R7) and (R9) increases (also evident in Fig. 2).

The direct and the effective yields do not differ significantly for water vapor throughout the stratosphere and most of the mesosphere. This suggests that the H₂O recycling at these pressure levels and chemical regimes is predominant, and all broken down water is regenerated. Nevertheless, in

the mesosphere at approximately 0.1 hPa, the effective yield decreases more strongly than the direct yield, reaching the minimum of 0.17 at 0.02 hPa, with a slight increase to 0.39 at the topmost layer at 0.01 hPa.

The value of 2 between 4 and 0.2 hPa reflects that all H from CH₄ reaches H₂O eventually at these altitudes, supporting the assumption as accepted in the literature. In the lower stratosphere and upper mesosphere, however, the box model results show that assuming a yield of 2 will lead to an overestimated H₂O production.

The yield of H₂ (see Fig. 3b) shows a mostly anticorrelated behavior with respect to the yield of H₂O. Throughout most of the stratosphere, the effective and direct yields of H₂ differ by about 0.2, while the effective yield drops down to 0 between 4 and 0.2 hPa, i.e., exactly in the region where the yield of H₂O attains its maximum. In accordance with the decreasing yield of H₂O, the direct and effective yields of H₂ increase substantially at higher altitudes, giving evidence that more and more H becomes diverted to and stays in H₂ instead of continuing towards H₂O.

A good indicator for the rate of general chemical reactivity in the atmosphere is the CH₄ lifetime, which is mostly influenced by both temperature and the concentration of the reaction partners. The lifetime of CH₄ (τ_{CH_4}) with respect to its sinks OH, Cl, O(¹D) and photolysis is defined as

$$\tau_{\text{CH}_4} = \frac{1}{(k_{\text{OH}} \cdot [\text{OH}] + k_{\text{Cl}} \cdot [\text{Cl}] + k_{\text{O}(\text{1D})} \cdot [\text{O}(\text{1D})]) \cdot c_{\text{air}} + j_{\text{CH}_4}}, \quad (5)$$

with k_X being the reaction rate coefficients of CH₄ + X in cm³ s⁻¹, [X] the mixing ratio of species X, c_{air} the concentration of dry air in molecules cm⁻³ and j_{CH_4} the photolysis rate of CH₄ in molecules s⁻¹.

The area where the H₂O yield attains its maximum, i.e., where it is 2, corresponds to the area where the lifetime of CH₄ attains its stratospheric minimum (see Fig. 4). However, the CH₄ lifetime does not fully explain the behavior of the chemical yield, since in the upper mesosphere both yield and lifetime drop to a minimum, which can be explained by the emerging role of photolysis in this area. This further suggests that OH is an important factor in the H₂O yield in the stratosphere but does not influence it alone. It becomes replaced by photolysis in the mesosphere, which influences the CH₄ lifetime and, more importantly, destroys H₂O and initiates its recycling.

A sensitivity study concerning the impact of OH on $\gamma_{\text{H}_2\text{O}}$ is presented in the next section.

3.1.2 Sensitivity with respect to OH

The results of the previous section reveal that the effective yield of water vapor from CH₄ oxidation depends on the box location and hence the chemical regime at a certain pressure level. Particularly, OH is one of the major oxidants shaping the chemical regime and largely controls the conversion of CH₄ to H₂ and H₂O, respectively. In the simulations shown

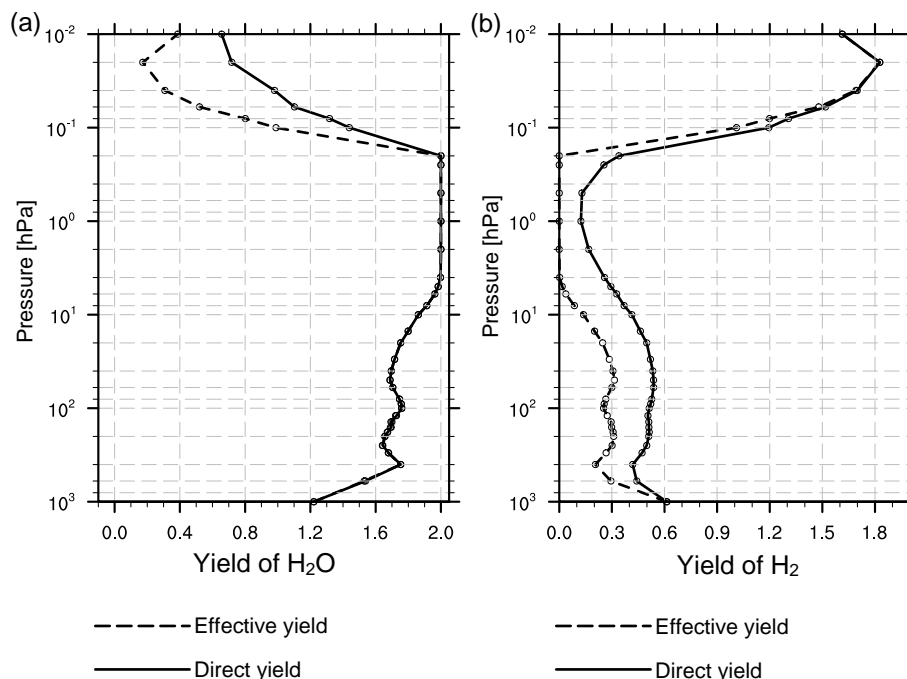


Figure 3. The pseudo-vertical profile shows the H₂O yield (a) and H₂ yield (b), calculated by the box model approach. The solid line represents the direct yield, the dashed line represents the effective yield, and circles indicate the pressure levels of the model boxes.

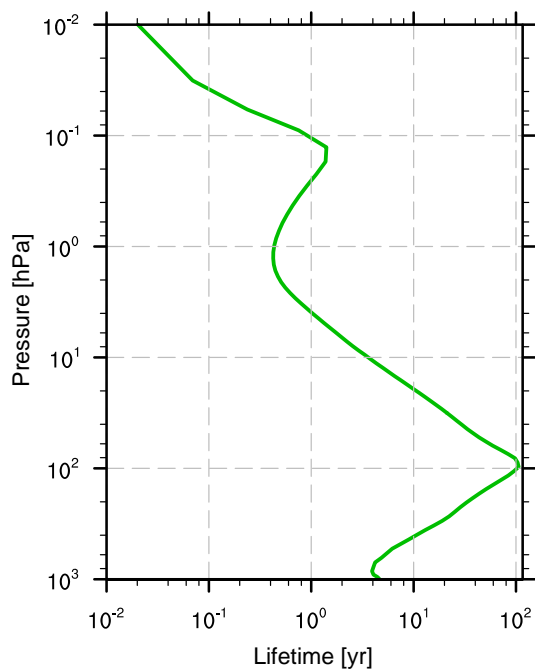


Figure 4. Vertical profile of CH₄ lifetime in the tropics with respect to removal by OH, O(¹D), Cl and photolysis in years.

above (Exp1), the OH is unconstrained; however, its final (equilibrated) OH concentration does not deviate much from the initial values (see Fig. 5). The following sensitivity study

aims towards understanding the relationship between the OH and the vertical profile of the yield. It is investigated whether the variations of the yield are directly related to OH variations or to other parameters.

In further sensitivity simulations with CAABA, OH is initialized with the reference from EMAC multiplied with constants and kept constant throughout the simulation. This introduces an additional prescribed hydrogen-carrying species, which introduces or withdraws hydrogen to or from the system. However, contribution of OH to the total H abundance in the system was found negligible. The first four simulations reduce the OH concentration by the factors of 0.5 (SS1), 0.1 (SS2), 0.05 (SS3) and 0.01 (SS4), respectively, while the fifth one is performed with a doubled OH concentration (SS5). One additional simulation represents the reference simulation (Ref), which started with an OH concentration identical to the analysis above, except that OH is kept constant. The simulations are listed in Table 2. The simulation setup uses extreme perturbations of the OH concentration to provide a qualitative estimate of the impact of OH on the H₂O yield from CH₄ oxidation.

The results of the sensitivity simulations are shown in Fig. 6. First of all, the initial experiment, Exp1 (see Fig. 3), and the reference experiment of the sensitivity study, Ref (see red line in Fig. 6), show mostly consistent results compared to each other concerning the effective and direct yields, which confirms that prescribing OH is adequate. However, in the upper mesosphere, where the OH concentration has the

Table 2. Overview of simulations carried out in this study, including box model simulations and the sensitivity study concerning H₂O yield dependence on OH as well as the global simulations with EMAC.

Name	Description	Simulation
Exp1	Experiment with unconstrained OH	Box model
Ref	Reference with standard fixed OH concentration from yearly climatology of RC1SD-base-07	Box model
SS1	Sensitivity simulation with $0.5 \times$ OH from Ref	Box model
SS2	Sensitivity simulation with $0.1 \times$ OH from Ref	Box model
SS3	Sensitivity simulation with $0.05 \times$ OH from Ref	Box model
SS4	Sensitivity simulation with $0.01 \times$ OH from Ref	Box model
SS5	Sensitivity simulation with $2.0 \times$ OH from Ref	Box model
Exp2	Global simulation with EMAC, MECCA and MECCA-TAG	CCM

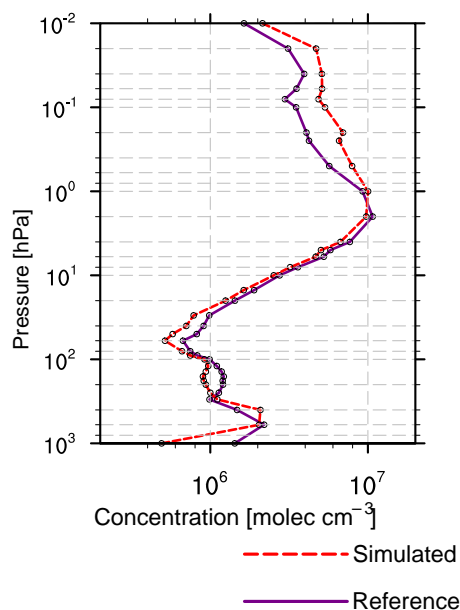


Figure 5. Reference OH concentration in the tropics from ESCiMo experiment RC1SD-base-07 (purple) and OH concentration as simulated in respective boxes (red).

largest difference (cf. Fig. 5), the effective yield in the experiment Ref drops already at 1 hPa significantly. Additionally, the effective yield in the experiment Ref reaches a value lower than the effective yield in the experiment Exp1 in this area. Nevertheless, the direct yield is not considerably different between these two experiments. This once more supports the assumption of a strong OH dependence of $\gamma_{\text{H}_2\text{O}}$.

Comparing experiment Ref with SS1 shows that reducing the OH concentrations by half reduces the direct and effective yields by about 0.05 in the lower stratosphere. Altogether, the direct yield profiles are rather similar in experiments Ref and SS1, with an exception of lower values in SS1 within the 10–1 hPa range and above 0.2 hPa. Prominent, however, is the difference in the effective yield. In the experiment SS1, the effective yield drops to zero already at

0.04 hPa and does not have the local enhancement seen in experiment Ref around 0.2–0.02 hPa.

Considering the sensitivity simulations SS2–SS4, the effect of OH reduction on $\gamma_{\text{H}_2\text{O}}$ becomes more apparent. The effective yield drops to zero already above 60 hPa. The direct yield shows strongly reduced values in the stratosphere, with a local minimum at 20 hPa for SS2 and SS3 and a bit above for SS4, being 1.08, 0.92 and 0.78, respectively. Above 20 hPa, the direct yield increases towards a local maximum at 2 hPa, following the profile of the CH₄ lifetime. Above 2 hPa, the direct yield decreases nearly monotonically.

In the experiment SS5, with doubled OH, $\gamma_{\text{H}_2\text{O}}$ is about 0.07 higher compared to experiment Ref and nearly replicates the results of experiment Exp1 in the mesosphere, where the OH equilibrated at a value of about twice that of the reference OH concentration from EMAC.

Compared to the yields of H₂O, the effective and direct yields of H₂ show moderate dependence on OH concentration. The yield of H₂ is rather constant at lower levels, reaches its minimum around the stratopause and increases again above that to its maximum. Around the stratopause and in the lower mesosphere, all experiments show similar results. In lower boxes, the simulations with lower OH show higher yields, and vice versa. In contrast to this, the boxes in the middle mesosphere and above show an inverted behavior, except, however, for experiment SS5, which results in a lower yield than in the reference simulation.

Moreover, profiles of the yield of H₂ from the oxidation of CH₄ (γ_{H_2}) of experiments SS2, SS3 and SS4 overall do not vary much compared to each other.

Summarizing, increasing OH concentrations lead to higher direct and effective H₂O yields. Both yields show a larger difference to the reference at higher altitudes with varying OH, indicating that the sensitivity of the chemical regime with respect to the OH concentration increases with altitude.

The results of the sensitivity study suggest that the effective yield of H₂O has a high sensitivity to the OH concentration and give evidence that a minimum OH concentration is required for an effective H₂O recycling.

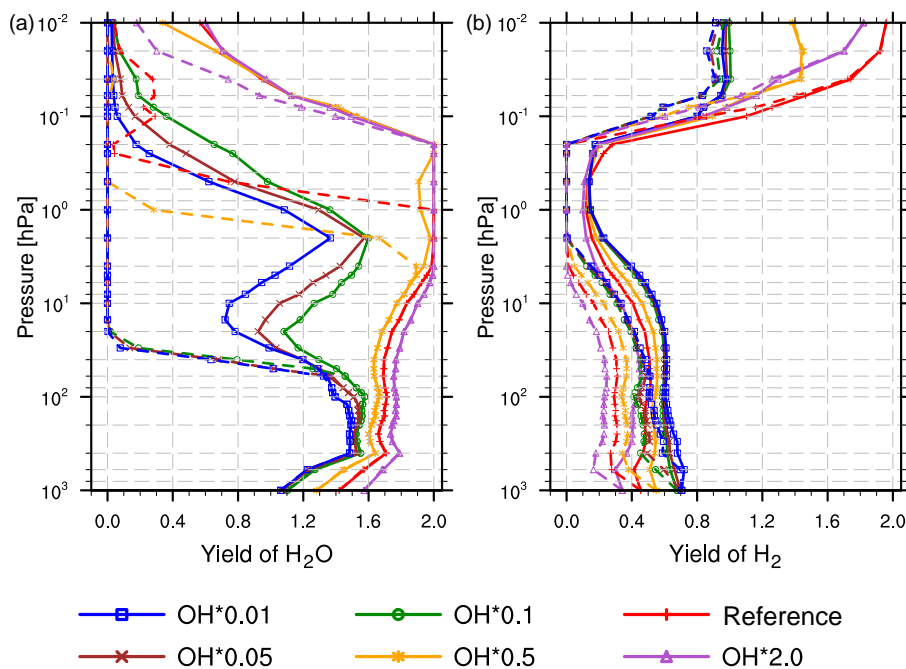


Figure 6. Pseudo-vertical profiles of the H₂O yield (a) and H₂ yield (b), calculated by the box model approach. Solid lines represent the direct yield, the dashed lines the effective yield and circles indicate the pressure levels of the model boxes. OH concentrations are prescribed in all simulations to the initial values of the respective vertical box. The plot shows simulations with the reference OH concentration (Ref, red, plus signs) as well as the OH concentration multiplied by 2 (SS5, purple, triangles), multiplied by 0.5 (SS1, orange, asterisks), multiplied by 0.1 (SS2, green, circles), multiplied by 0.05 (SS3, brown, crosses) and multiplied by 0.01 (SS4, blue, squares).

The γ_{H_2} shows an anticorrelated behavior to that of the H₂O yield, however, as an exception; doubling of OH shows a lower yield than the reference in the mesosphere.

3.1.3 Dependencies on pressure and temperature

The results shown in the previous subsection indicate that there is an OH dependence in both the effective and direct yield. To investigate whether this dependency is systematic, simulated H₂O yields are plotted as $\gamma_{\text{H}_2\text{O}}$ versus OH mixing ratio in Fig. 7. Generally, there is no linear correlation between these two parameters. However, a systematic dependence is evident for each box, i.e., at each pressure level. The slope of the correlation is thereby dependent on the pressure level. For higher pressure, the gradient is low and becomes steeper for lower pressure levels.

The slope of the correlation of OH and the direct yield (see Fig. 7a) is smaller for pressure levels at 2–80 hPa than the slope of the effective yield (see Fig. 7b) at corresponding pressure levels. Moreover, the effective yield has a sharp transition from low to high OH values, while the direct yield increases more gradually.

The scatterplots give evidence that in a certain range of pressure levels the yields exhibit a saturation-like behavior with respect to OH concentrations. Furthermore, there is no indication of a connection between the yield-OH dependence and the temperature (see Fig. 8 and the non-ordered colors in-

dicating the temperature), despite the fact that reaction rates in the CH₄ → H₂/H₂O cycle are usually stronger impacted by temperature than by pressure.

We carried out additional sensitivity studies in order to investigate the temperature dependence of the yield on a given pressure level. Results are displayed in Fig. 9. The simulation setups are identical to that of experiment Ref, except that temperature in every box was varied within –15 to +15 K with 5 K steps. This temperature range is chosen as it represents a range exceeding day–night differences (less than ±5 K) and the annual cycle (less than ±10 K) in the tropics. In the lower stratosphere, there is no indication of a significant temperature sensitivity of the effective and direct yields. The latter also does not show any significant sensitivity at higher altitudes. The effective yield in the upper stratosphere and mesosphere shows a small dependence in a way that lower temperatures increase the yield, and vice versa.

Consideration of the obvious vertical dependence and the very low temperature dependence gives evidence that not the physical parameters (temperature and pressure) themselves are crucial for the H₂O yield but rather the chemical composition of the box (i.e., among others, abundances of OH, HO₂, O(¹D) and Cl). This chemical composition, however, changes with altitude (hence with pressure) and depends additionally on transport.

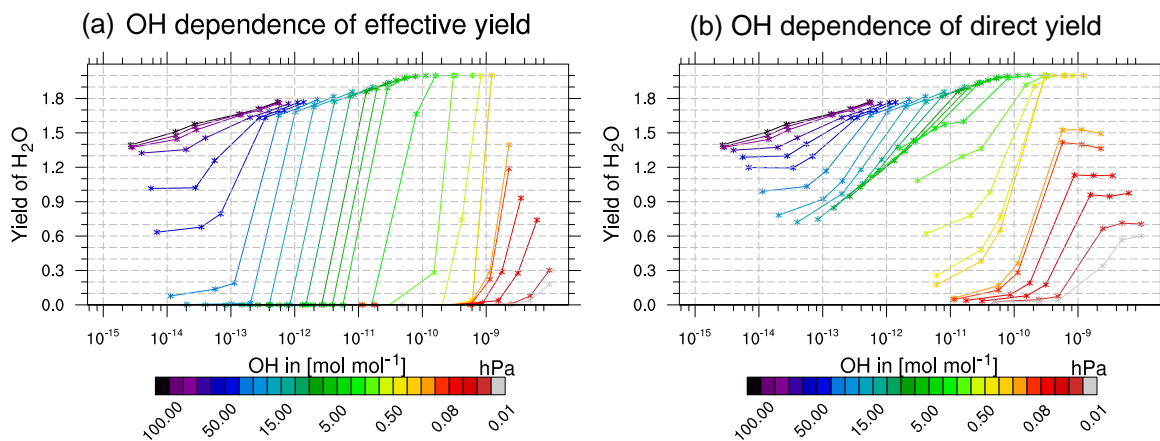


Figure 7. Effective yield (a) and direct yield (b) versus OH; colors indicate pressure level from low to high pressure.

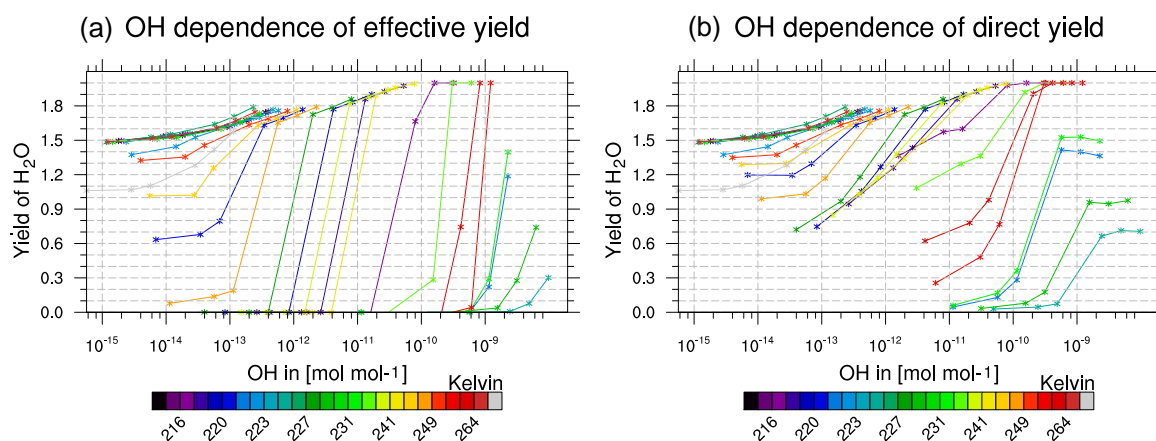


Figure 8. Effective yield (a) and direct yield (b) versus OH; colors indicate temperature from low to high temperature.

3.2 Global model approach

As stated before, the box model approach does not take into account vertical transport and requires certain assumptions. Consequently, the boxes do not fully represent atmospheric conditions. To investigate the production of SWV in a comprehensive setup, MECCA-TAG is applied in a global simulation with EMAC. The full chemistry of MECCA plus MECCA-TAG, which more than triples the amount of simulated tracers, increases the computational demands substantially. The additional tracers in the model defined by MECCA-TAG are basically counterparts of the tracers of the regular chemical mechanism and are marked (tagged) to be distinguishable from each other. In the following, these tracers are indicated by the label “tagged”. A spin-up simulation of 6 years with a reduced vertical resolution is carried out to pre-adjust tagged tracers. The results shown here originate from a subsequent simulation, which is executed for another 2-year model time.

Although the global simulation provides a three-dimensional field, we focus in the current study on the vertical zonal mean profile of the yield of H₂O from CH₄ oxidation ($\gamma_{\text{H}_2\text{O}}$) averaged over the tropics. An analysis of the zonal mean without meridional averaging (see Fig. S1 in the Supplement) shows that the conclusions presented in this section also apply to a certain degree at midlatitudes. In the polar regions, the analysis of the calculated yield is not useful as long periods without sunlight, and hence photolysis introduces substantial numerical errors into the calculation of $\gamma_{\text{H}_2\text{O}}$.

Figure 10 shows the vertical profile of the direct and effective yield of H₂O in the tropics (23° S–23° N). Both match the vertical profile of the results of the box model simulation Exp1 superficially. However, there are certain differences.

First, the yield of H₂O from CH₄ oxidation increases in the upper stratosphere and lower mesosphere to a value above 2, because the global model, unlike the box model, includes vertical transport. The tagged intermediates which are produced at lower levels are transported upward and are finally converted

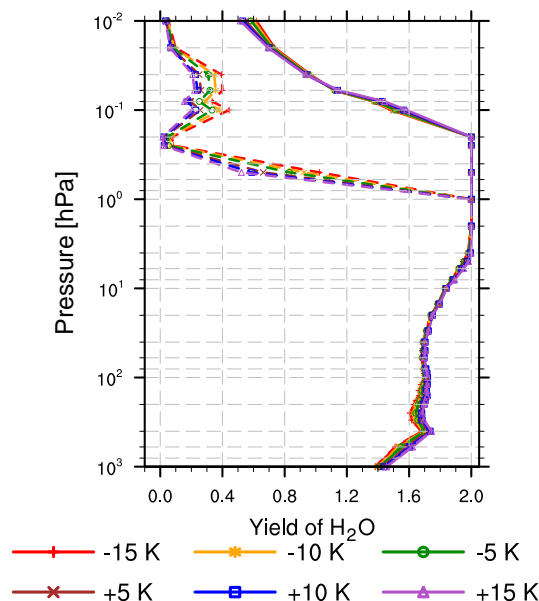


Figure 9. The pseudo-vertical profile of the H₂O yield calculated by the box model approach. Solid lines represent the direct yield, the dashed lines the effective yield and circles indicate the pressure levels of the model boxes. OH is kept constant to the initial values of the respective vertical box. The plot shows sensitivities concerning temperature. Temperature is varied from the standard atmosphere value by -15 K (red), -10 K (orange), -5 K (green), $+5$ K (brown), $+10$ K (blue) and $+15$ K (purple).

to H₂O. The by far most abundant intermediate is tagged H₂ with about $0.25 \mu\text{mol mol}^{-1}$ at 0.2 hPa. Hydrogen gas has a comparably as long lifetime as CH₄, since it is reacting with the same species and comparable reaction rates (Rahn et al., 2003; S. P. Sander et al., 2011). The transported tagged H₂ reacts further to H₂O. This results in a production of more than two H₂O molecules per oxidized CH₄ in one specific layer, because this additional production is counted as well. In layers where the increased production takes place, high OH concentration supports the conversion of the intermediates towards H₂O, since OH is the main driver of the chemistry (e.g., $\text{H}_2 + \text{OH} \rightarrow \text{H}_2\text{O} + \text{H}$).

The three topmost model layers in the upper mesosphere (0.06–0.01 hPa) are possibly subject to artifacts due to the nearby top of the global model and are therefore not considered in this analysis. It is assumed that the trend, which is evident below 0.1 hPa, showing decreasing $\gamma_{\text{H}_2\text{O}}$ values also applies to the upper mesosphere, which would be similar to the box model results in the section above.

In Fig. 11, it also becomes obvious that the loss of H₂O increases at higher altitudes. Additionally, the recycling of H₂O contributes considerably to the effective yield. The photooxidation of H₂O drives the continuous recycling of H₂O to H₂ and back, shifting the equilibrium between these two gases towards H₂.

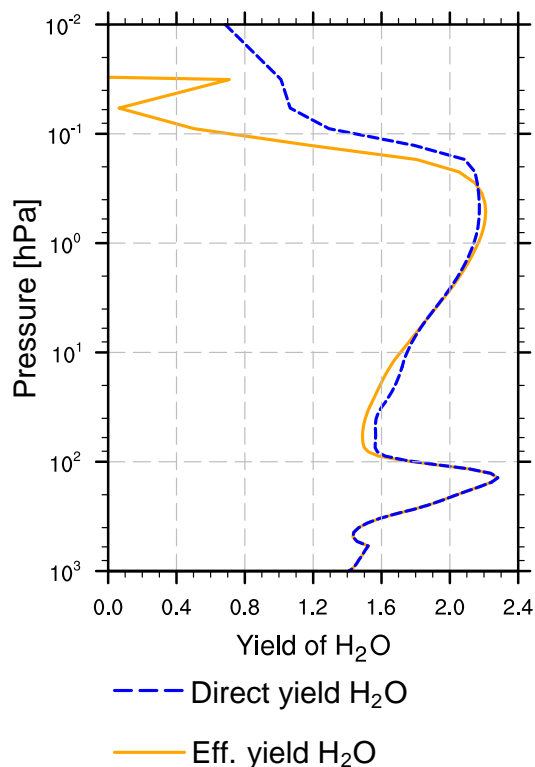


Figure 10. Effective and direct yield calculated from results of the global simulation in the tropics (23° S– 23° N).

Altogether, the separated H₂O and H₂ loss/production terms of the global model are consistent with the box model findings. They also show a local maximum in loss of CH₄ and primary production of H₂O below the stratopause and the strongly pronounced secondary loss and production of H₂O in the middle and towards the upper mesosphere.

3.3 Ratio of H : H₂ : H₂O

A different approach than the first two presented ones to determine $\gamma_{\text{H}_2\text{O}}$ in the stratosphere is to use the fact that the vertical profile of the H content in terms of atoms is fairly constant above the tropopause (see Fig. 12a) compared to tropospheric variations. The H content in the stratosphere consists mostly of CH₄, H₂O, H₂ and, in the topmost layers, H. Other H-carrying substances, such as OH and HNO₃, can be neglected for the H budget. The chemical regime determines the proportion between H, H₂ and H₂O, but the total H content is preserved. Figure 12b shows the tagged H content in the same manner. In this panel, the difference between the total H₂ including the transported H₂ from the troposphere, which is observed in atmospheric measurements, and the H₂ solely produced by CH₄ becomes distinguishable. The contribution of H₂ produced from methane increases with altitude (corresponding to $\gamma_{\text{H}_2\text{O}} < 2$), whereas the H₂ originally injected from the troposphere decreases (by oxidation into

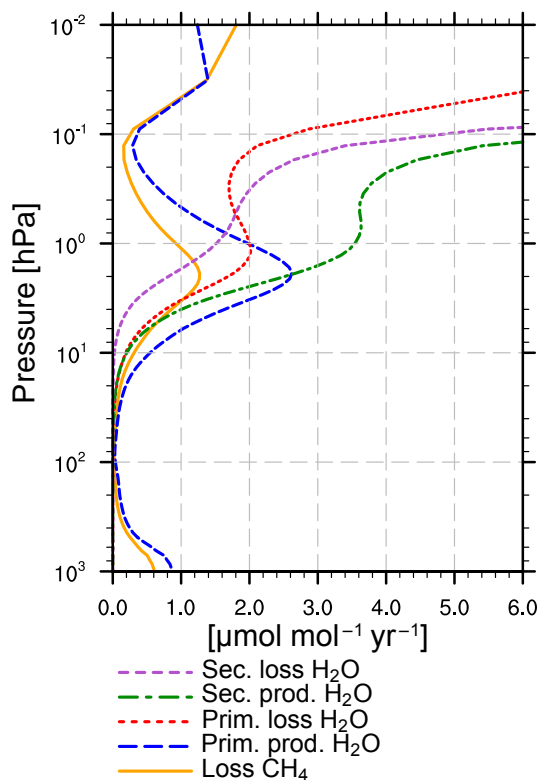


Figure 11. Separate loss of CH₄ and primary and secondary loss and production of H₂O from the global simulation (23° S–23° N).

H₂O). Therefore, the net H₂ content is (almost) constant, at least in the lower stratosphere where measurements are available.

The effective yield of H₂O from CH₄ oxidation, as explained in previous sections, describes the net production of H₂O. Precisely, it is an indicator for the interaction of loss and production of H₂O, further influencing the production of H₂ and H as well. As a first assumption, additional H from CH₄ oxidation should be partitioned to the reservoirs of H, H₂ and H₂O in the same proportion as is present in the steady state. This is based on the supposition that it does not matter whether the H, which is injected to the hydrogen cycling and reaches the indicated H reservoirs, comes from CH₄ or any other hydrogen supply. If we assume further that CH₄ is at higher layers the only additional hydrogen supply, we can determine the effective yield of H₂O by CH₄ oxidation through the proportion of annually averaged H atoms in H₂O to the total hydrogen content of H, H₂ and H₂O. This proportion of the total hydrological content is subsequently called the H portion of H₂O.

In Fig. 13, the H portion of tagged and total H₂O is plotted with respect to the sum of tagged and total hydrogen content in the CH₄ oxidation products H, H₂ and H₂O, from the global experiment Exp2. This sum (H + 2 · H₂ + 2 · H₂O + 4 · CH₄) of 15 μmol mol⁻¹ is in accordance with the estimate

derived with the CHEM2D model by Wrotny et al. (2010) for the sum of H₂ + H₂O + 2 · CH₄ being ~ 7.5 μmol mol⁻¹ (i.e., one-half of ~ 15 μmol mol⁻¹). The individual abundances of H₂, H₂O and CH₄ also agree well with each other.

The H portion of H₂O in the hydrogen budget is 2 in the troposphere and decreases to a minimum right above the tropopause. The hydrological cycle is producing a generally humid troposphere. Therefore, H₂O in the lower layers of the atmosphere is prevailing versus H₂ and H, which are quickly oxidized as soon as they are produced. The minimum of the H portion of H₂O above the troposphere can be explained by the freeze drying at the cold point. This reduces the H portion of H₂O versus the one of H and H₂.

This minimum is not equally plain in the tagged H₂O. Note that tagged H₂O in the troposphere is already lower than the total H₂O, since it is solely produced by CH₄ oxidation. When CH₄ ascends from the troposphere through the cold point into the stratosphere, it continuously produces H₂O, although at low rates (due to low temperatures). Therefore, tagged H₂O is still produced by CH₄ and even though it partly freezes out, the proportion to H and H₂ is not much impacted. However, in the lower stratosphere, the mixing ratio of tagged H₂ increases, while H₂O is still restrained by the cold point. This behavior becomes more apparent in the case of the tagged species, since their absolute amounts are fairly low compared to the total ones.

Nevertheless, the H portion of tagged H₂O and total H₂O behave similarly above the minimum at the tropopause, as seen in the maximum around the stratopause and in the lower mesosphere and the strong decrease in the middle mesosphere and above. The general behavior of the vertical profile also agrees well with the above findings of the yield calculations using box model and global model results.

4 Discussion

The presented results show three different approaches in estimating $\gamma_{\text{H}_2\text{O}}$. Taking the results of the separate approaches together gives the opportunity to discuss certain processes which are differently parameterized and decisive for the yield estimation. We first want to discuss the general benefits and limitations of the approaches.

In the box model, we have the opportunity to study a chemical regime without transport. It enables us to solely assess the involved chemical kinetics. Clearly, the box model chemistry does not fully represent the intended atmospheric conditions. Setting certain species to a constant value does change the chemical regime. However, without constraints on the chemical species, the model would run into a new equilibrium, which changes the regime as well. It therefore needs careful weighing to specify which species should be kept constant and which species should be allowed to re-adjust, to be able to simulate a representative chemical regime.

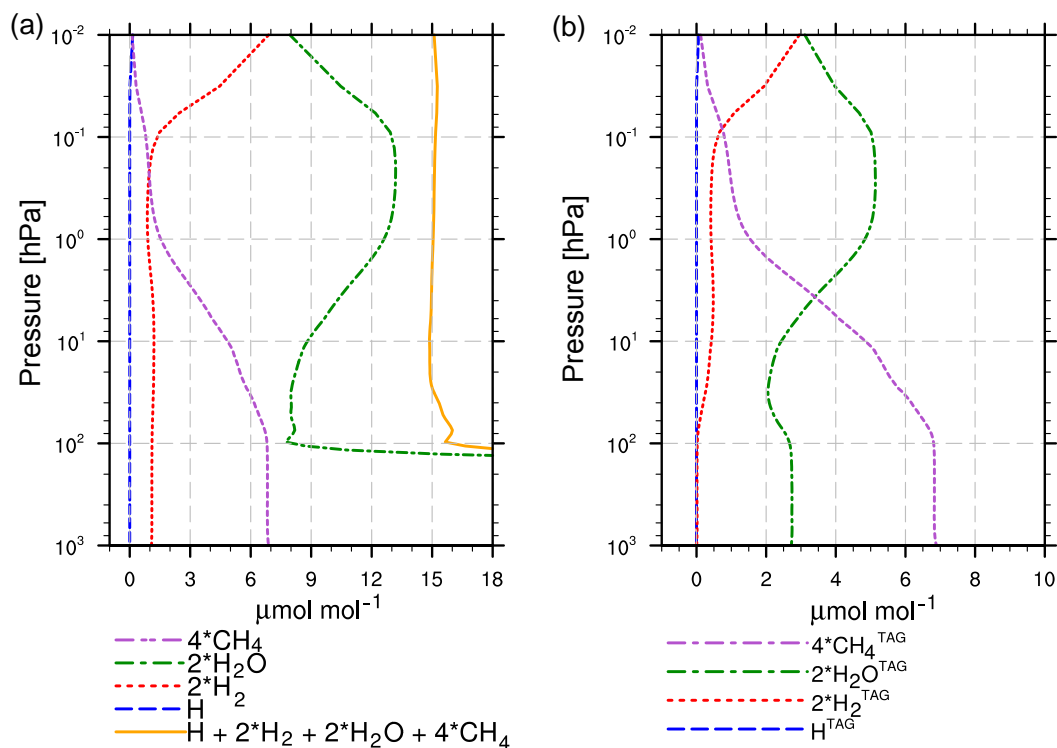


Figure 12. Annual zonal average of general H (a) and tagged H (b) content by species (in $\mu\text{mol mol}^{-1}$) over the tropics (23°S – 23°N).

In the global model, we are not restricted to one vertical profile but can evaluate the yield in three dimensions. Nevertheless, the effects of transport and chemical regime on the yield cannot be separated, since transport influences the chemical regime. The vertical profile of $\gamma_{\text{H}_2\text{O}}$ is for this reason susceptible to changes in dynamical processes as, for example, the Brewer–Dobson circulation.

The third approach, which used the total H budgets and portions, helps to quantitatively evaluate the methods, which are calculating the effective yield. It shows the actual portion of hydrogen from CH₄ in the total hydrogen without a production and loss term, which is sensitive to variations in the chemical regime. Yet, this approach is not directly linked to the loss of CH₄ and it is not possible to explicitly resolve the influence of chemistry, since, for example, it is not clear if the decreasing values of $\gamma_{\text{H}_2\text{O}}$ in the mesosphere are due to the increasing loss of H₂O or due to the reduced oxidation of CH₄.

Figure 14 shows the vertical profiles of the H₂O yields and H portions calculated by the approaches described in the previous sections combined in one plot.

Comparing the results of the box model and the global model in the lower stratosphere, $\gamma_{\text{H}_2\text{O}}$ in the global model is lower than in the box model. This suggests that CH₄-produced H₂O is transported into the stratosphere, where it is destroyed, adding to the loss of H₂O. This reduces $\gamma_{\text{H}_2\text{O}}$ while the oxidation of CH₄ is low, due to the exception-

ally long lifetime of CH₄ due to low temperatures and low OH concentrations. In the upper stratosphere, global model $\gamma_{\text{H}_2\text{O}}$ is larger than box model $\gamma_{\text{H}_2\text{O}}$ and, more importantly, larger than 2, which is attributed to transport. This time, CH₄-derived intermediate H₂ molecules are elevated and produce H₂O independent of the CH₄ oxidized in this region. This contradicts the assumption that two H₂O molecules are immediately produced from CH₄ oxidation, since intermediates, specifically intermediate H₂ molecules, do play an important role. This is furthermore consistent with the findings of Wrotny et al. (2010), who calculated a yield larger than 2 in this area as well. However, our results are lower than those from Wrotny et al. (2010). As they stated in their conclusions, “the net loss of H₂ [...] drives additional H₂O production, thus producing positive vertical gradients in H₂O + 2 · CH₄” (Wrotny et al., 2010). In other words, they attribute the values above 2 to the production from H₂. Our method distinguishes H₂ produced by CH₄ oxidation from H₂ from other sources (e.g., transport from the troposphere) and our yield is only defined for the CH₄ originating part. Therefore, it is lower than reported by Wrotny et al. (2010).

In the middle mesosphere, box model and global model $\gamma_{\text{H}_2\text{O}}$ values decrease substantially. Although the topmost layers must be considered with caution due to potential artifacts, it is possible that the yield of the global model reaches values below zero. In the global model, tagged H₂O is transported into the mesosphere, where it is destroyed, due to the

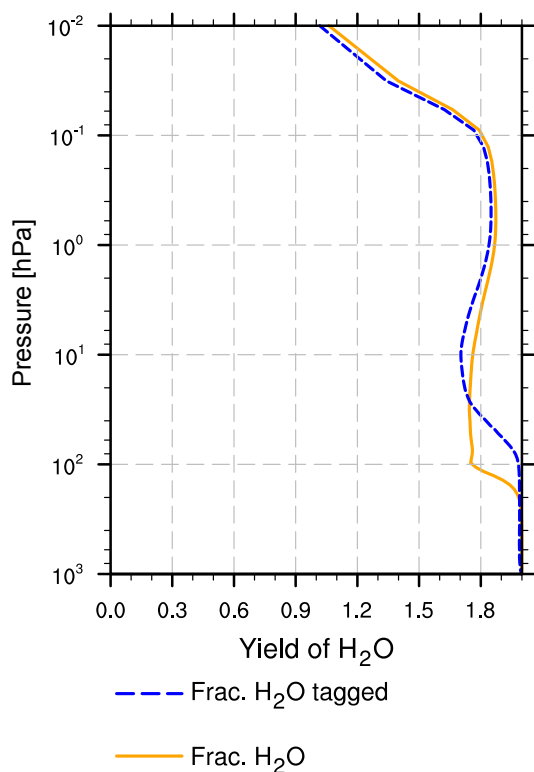


Figure 13. H portion of tagged and total H₂O with respect to the tagged and total hydrogen content $H_y = (H + 2 \cdot H_2 + 2 \cdot H_2O)$, respectively, i.e., $2 \cdot H_2O/H_y$ (orange solid) and $2 \cdot H_2O_{\text{tagged}}/H_{y_{\text{tagged}}}$ (blue dashed).

enhanced sink of H₂O through photooxidation. The effective yield decreases below zero, since the loss of H₂O becomes larger than the production of H₂O ($P_{H_2O}^I + P_{H_2O}^{II} < L_{H_2O}^I + L_{H_2O}^{II}$). This emphasizes the importance of H₂O destruction at higher altitudes, which particularly is not included, when parameterizing the chemical γ_{H_2O} of H₂O with two H₂O molecules per CH₄ molecule oxidized.

Moreover, the effective yield in the box model setup with fixed OH profile drops down at 1 hPa, while the yield of the box model with variable OH (Exp1) and the global model (Exp2) do not drop until 0.2 hPa. Additionally, Exp1 and Exp2 agree well concerning the altitude of the drop (the peak in Exp2 (red line) is most likely an artifact as discussed in Sect. 3.2). This suggests further that the chemical regime of the box model presented by the annual mean of the reference simulation (Ref) is not consistent with the chemical regime at the corresponding altitude concerning OH. The initialized and fixed value of OH at these levels is too low to realistically capture the chemical situation. This also shows that unconstrained OH is crucial and that the vertical profile of OH of simulation Exp1 in this region better agrees with the OH in the global simulation Exp2.

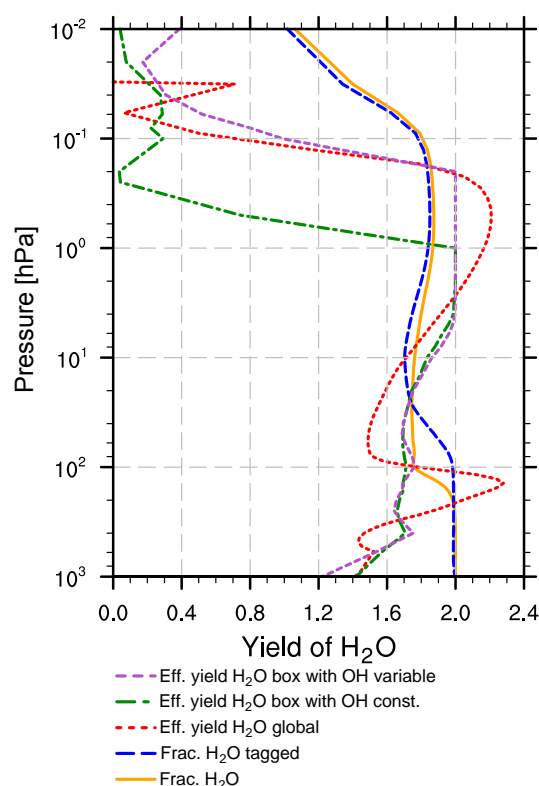


Figure 14. Comparison of all approaches determining the H₂O yield: effective yield by box model simulations with variable OH (purple, dashed) and fixed OH (green, dash dotted), effective yield by global model simulations (red, dotted), H portion of total (yellow, solid) and tagged (blue, long dashed) H₂O with respect to the hydrogen content.

The H portion of H₂O in the hydrogen content matches qualitatively the results of the yield calculations in the box and global model approaches. MECCA-TAG again enables us to focus on H in H₂O particularly from CH₄ oxidation and to ignore the H from other sources. The minimum of the H portion of H₂O in the lower stratosphere and its maximum close to the stratopause and in the lower mesosphere therefore show that the production of H₂O from CH₄ oxidation relative to the production of H₂ from CH₄ oxidation is smaller in the lower stratosphere and becomes larger towards the upper stratosphere. Accordingly, we conclude that our estimation that γ_{H_2O} differs significantly from 2 in the lower stratosphere is reliable.

Altogether, the different approaches yield consistent results. All suggest a yield of less than 2 in the lower stratosphere, varying between 1.5 and 1.7. The smallest value is estimated in the global simulation Exp2, where the yield is larger than the one of le Texier et al. (1988), which is $\gamma_{H_2O} = 1.3$ at corresponding altitudes. The results of le Texier et al. (1988) also showed a maximum around 1 hPa, which is consistent with our results, albeit a bit above 1.8 and with

that lower than our estimate of 2 (or more in the case of the global simulation) in that region.

Overall, the estimated yield of H₂ from le Texier et al. (1988) and the yield of H₂ estimated by the box model approach are consistent as well. While our resulting $\gamma_{\text{H}_2\text{O}}$ is larger than in le Texier et al. (1988), the γ_{H_2} is lower. Still, the vertical profiles of γ_{H_2} in both studies are comparable.

The fundamental study of le Texier et al. (1988) does not capture the influence of the increasing loss of H₂O at higher altitudes. They only considered the direct yield of H₂O and do not include H₂O loss in their calculation. Nevertheless, the findings in our study show that the difference between effective and direct yield becomes only apparent above 0.1 hPa, and le Texier et al. (1988) do not discuss results above this pressure level.

Furthermore, le Texier et al. (1988) is often cited as the reference for the assumption of $\gamma_{\text{H}_2\text{O}} = 2$. However, in the lower stratosphere, our results and those of le Texier et al. (1988) actually agree that $\gamma_{\text{H}_2\text{O}}$ is less than 2, which objects to the assumption of a constant $\gamma_{\text{H}_2\text{O}} = 2$.

Hurst et al. (1999) calculated a net production of H₂O of 1.973 ± 0.003 , which includes a loss of H via H₂ of 0.027 ± 0.003 . These values differ from our findings in the box model approach. Our estimated $\gamma_{\text{H}_2\text{O}}$ is smaller and our γ_{H_2} is larger than those estimated by Hurst et al. (1999). As noted before, by using observational data, it is not possible to distinguish between H₂ from the troposphere and H₂ produced by H from CH₄, which results in this rather low net production of H₂. Assume, for example, that H₂ is not produced in the stratosphere. The mixing ratio of H₂ will then decrease with respect to altitude. However, the contribution from CH₄ oxidation to H₂ fills up the oxidized molecules, and only if $\gamma_{\text{H}_2} \cdot [\text{CH}_4]$ is larger than the total loss of H₂, observed H₂ and CH₄ are anticorrelated. Using the kinetic tagging gives us the opportunity to distinguish between the total loss of H₂ and the loss of those H₂ molecules carrying H from CH₄. Our findings therefore provide additional insight into processes which determine the observed vertical profiles and provide estimates for the contribution of CH₄ separated from the background H₂ and H₂O.

The study of Wrotny et al. (2010), based on a correlation analysis of satellite measurements, derived a yield of 2.6–2.7 at 1.0 hPa (depending on the satellite product and error assumptions). These are larger than our estimate, which is less than 2.3. Nevertheless, we agree that the yield can be larger than 2, but a direct comparison of our model results with the measurement-based derivation of Wrotny et al. (2010) is not possible for the arguments given above.

Summarizing, our results suggest that applying $\gamma_{\text{H}_2\text{O}} = 2$ as the contribution to H₂O by the oxidation of CH₄ in climate models likely overestimates the kinetic yield of H₂O in the lower stratosphere and in the mesosphere above 0.2 hPa.

Based on our simulations, in the lower stratosphere between 100 and 10 hPa, the portion of H₂O from CH₄ is in the range of 25 to 44 % (calculated in Fig. 12 by taking the ratio

of tagged and total H₂O). Assuming $\gamma_{\text{H}_2\text{O}} = 2$ overestimates the contribution of CH₄ oxidation to the H₂O production by 10 to 25%, which is equivalent to an overestimation of total water of 2.5 up to 11 %. Given the large uncertainties of H₂O measurements in this altitude range and the high sensitivity for climate impact (Solomon et al., 2010), a 10 % change in water vapor can have a measurable impact. This impact can only be estimated by sensitivity climate simulations. These are, however, beyond the scope of our present study.

We admit that a small fraction of H₂O should also be produced from H₂ ascending from the troposphere. This likely reduces the SWV bias in GCM simulations using the approximation of $\gamma_{\text{H}_2\text{O}} = 2$, since those models do not include a separate H₂O production from H₂ oxidation. Nevertheless, to be punctilious, the yield of H₂O from CH₄ oxidation should be distinguished from the net chemical production of H₂O. In subsequent studies, we intend to apply the tagging method for estimating a $\gamma_{\text{H}_2\text{O}}$ from H₂ oxidation ($\gamma_{\text{H}_2\text{O}}(\text{H}_2)$). H₂ and CH₄ may oxidize at a similar rate, but the resulting products are different, which likely results in a varied $\gamma_{\text{H}_2\text{O}}$ with respect to the source gas (i.e., $\gamma_{\text{H}_2\text{O}}(\text{CH}_4) \neq \gamma_{\text{H}_2\text{O}}(\text{H}_2)$).

4.1 Recommendations for GCMs without online chemistry

An important disadvantage of the parameterization as in Eq. (1) with $\gamma_{\text{H}_2\text{O}} = 2$ is that it does not account for the loss of H₂O in the mesosphere. Even though CH₄ oxidation becomes negligible at these altitudes, this simple parameterization does not consider that H₂O gets chemically destroyed. Strictly speaking, the loss of H₂O is independent of CH₄ and should potentially be included separately. MacKenzie and Harwood (2004) and McCormack et al. (2008) presented, for example, sophisticated parameterizations, which target this issue in their 2-D atmospheric models. Based on our results, we recommend to apply a parameterization, which is not solely based on the loss of CH₄ but accounts for the reduced yield in the lower stratosphere and also includes the loss of H₂O.

Besides this, transport of intermediate H₂ molecules is an important factor for the vertical profile of the $\gamma_{\text{H}_2\text{O}}$. It must be noted that atmospheric transport is not constant in time. The Brewer–Dobson circulation, for example, changes in future climate projections (Butchart et al., 2010). A simple parameterization of $\gamma_{\text{H}_2\text{O}}$ cannot take these changes in transport into account, since they depend on various factors. This raises indeed the question of whether a simplified parameterization of $\gamma_{\text{H}_2\text{O}}$ is at all applicable for future climate projections, or if it is necessary to simulate the full chemistry for an accurate representation of SWV. The need for online chemistry for meaningful climate projections has already been shown, e.g., by Chiodo and Polvani (2017) for a realistic response of Southern Hemisphere (SH) circulation to CO₂ changes.

Keeping these challenges in mind, we are interested in deriving a parameterization as an intermediate stage between

the very simple constant yield and the online chemistry. This is beyond the scope of the current study. Nevertheless, in the paragraph below, we provide a sketch of such a parameterization together with its limitations and requirements.

One could start with a parameterization as introduced by Eq. (1), however, with a pressure p (and latitude ϕ) dependent $\gamma_{\text{H}_2\text{O}}(p, \phi)$ derived from our vertical yield profiles. This adds a vertical dependency to the chemical production of H₂O per CH₄ oxidized. As long as no large variations or trends in the stratospheric transport are expected within the simulation period, our profile is a good approximation. The limitation is, however, that the pressure (and latitude) dependence is likely to change with changing climate.

At higher altitudes (above 0.2 hPa), the yield in Eq. (1) could be replaced or supplemented by an explicit parameterization of the chemical loss of H₂O, mostly via photolysis and the reaction with O(¹D); see MacKenzie and Harwood (2004) and McCormack et al. (2008). In the simplified methane chemistry of EMAC, for example, a predefined O(¹D) is also used for the reaction with CH₄ and could be reused for the reaction with H₂O. Again, the same limitation holds: under climate change, water vapor, and photolysis rates are likely to change.

Furthermore, for the sake of completeness concerning the chemical source of SWV, the contribution of H₂ transported from the troposphere into the stratosphere needs to be included as well. This requires at least one additional tracer for H₂ and a parameterization of the vertical profile of $\gamma_{\text{H}_2\text{O}}$ from troposphere-originated H₂ oxidation.

Last but not least, we doubt that a simple three-tracer (H₂, H₂O, CH₄) parameterization will be possible without a nearly full chemical mechanism, because the oxidation rates are largely dependent on ozone. Such an approach will hardly be meaningful for climate simulations.

5 Conclusions

In this study, we present a comprehensive evaluation of current assumptions and estimates of the chemical yield of H₂O from CH₄ oxidation in the middle atmosphere. We show results of three different approaches to estimate $\gamma_{\text{H}_2\text{O}}$ and discuss certain advantages and challenges.

We conclude that the widely used assumption that one CH₄ molecule produces two water molecules overestimates the kinetic H₂O production in the stratosphere up to 4 hPa and in the mesosphere above 0.2 hPa. Our results show that a local yield larger than 2 in certain areas is possible through ascended intermediate H₂ molecules. In addition to that, transport is generally an issue when dealing with kinetic yields, since it influences the chemical regimes at all altitudes. It also makes the interpretation of the presented approaches challenging, when these are investigated separately.

Nevertheless, the separate approaches presented in this study show consistently that $\gamma_{\text{H}_2\text{O}}$ is substantially lower than

2 in the lower stratosphere, has a local maximum between 0.2 and 0.4 hPa, and is exceedingly low in the upper mesosphere. We find a low $\gamma_{\text{H}_2\text{O}}$ in the middle and upper mesosphere, since the loss of H₂O at higher altitudes increases, shifting the equilibrium between H₂O and H₂ towards H₂. The chemical loss is therefore a crucial factor for the correct parameterization of SWV production from CH₄ oxidation. At some point, the loss of H₂O is so strong that H₂O is effectively destroyed per oxidized CH₄.

An additional result from the box model simulation is that the chemical yield of H₂O depends on the OH concentration and more generally on the chemical kinetics. A strong temperature dependence, however, could not be detected.

Furthermore, the presented results agree with earlier kinetic estimates of $\gamma_{\text{H}_2\text{O}}$ from le Texier et al. (1988), who state that not exactly two molecules are produced from CH₄ oxidation. Furthermore, our results give additional insight into observations (e.g., Hurst et al., 1999; Rahn et al., 2003), which are limited in detecting the chemical origin of H₂O.

Overall, the results of the separate approaches give evidence that calculating the yield of H₂O from CH₄ oxidation requires the loss of H₂O to be taken into account, making the task of creating a simple parameterization challenging. The latter also requires to admit a critical amount of assumptions about uncertain factors for an adequate atmospheric simulation. We therefore recommend, in order to maintain as much certainty as possible concerning the chemical yield of H₂O, to implement a simplified H₂O chemistry including the most important reactions determining the H₂O yield. The extent of the resulting subset of the chemical mechanism is determinative for the correct representation of the H₂O content in the middle atmosphere. However, it must be noted that a set of reactions required for the comprehensive simulation of H₂O kinetics is not substantially different from the one incorporated in the full chemistry setup and is therefore less beneficial in terms of computational resources than a parameterized model. Nevertheless, as stated before, a too simple parameterization introduces uncertainties, which makes it challenging to preserve the required accuracy for applications in the simulation of climate projections, where atmospheric dynamics (e.g., the Brewer–Dobson circulation) and chemistry potentially differ from the present-day atmosphere.

The investigations presented in this study should serve as a basis for future studies concerning the chemical yield of H₂O in the stratosphere and mesosphere. The gained knowledge can be used to derive new parameterizations of the chemical yield of H₂O for a potential application in GCMs.

Code and data availability. The Modular Earth Submodel System (MESSy) is continuously developed and applied by a consortium of institutions. The usage of MESSy and access to the source code are licensed to all affiliates of institutions, which are members of the MESSy Consortium. Institutions can become a member of the MESSy Consortium by signing the MESSy Memorandum of Un-

derstanding. More information can be found on the MESSy Consortium website (<http://www.messy-interface.org>). The data of the box model simulations described above are available in the Supplement. Data of the global simulation are available upon request from the corresponding author. We used the NCAR Command Language (NCL) for data analysis and to create some of the figures of this study (UCAR/NCAR/CISL/TDD, 2017).

The Supplement related to this article is available online at <https://doi.org/10.5194/acp-18-9955-2018-supplement>.

Author contributions. FF and SG prepared the model configurations and conducted the simulations. All authors contributed to the interpretation of the results and to the text.

Competing interests. The authors declare that they have no conflict of interest.

Acknowledgements. We acknowledge the DLR internal project KliSAW (Klimarelevanz von atmosphärischen Spurengasen, Aerosolen und Wolken), which provided the financial basis for the presented study.

The model simulations have been performed at the German Climate Computing Centre (DKRZ) through support from the Bundesministerium für Bildung und Forschung (BMBF).

We furthermore thank all contributors of the project ESCiMo (Earth System Chemistry integrated Modelling), which provides the reference profiles and initial conditions, as well as Christoph Kiemle for his internal review and valuable comments on the manuscript.

The article processing charges for this open-access publication were covered by a Research Centre of the Helmholtz Association.

Edited by: Jens-Uwe Grooß

Reviewed by: three anonymous referees

References

- Austin, J., Wilson, J., Li, F., and Vömel, H.: Evolution of Water Vapor Concentrations and Stratospheric Age of Air in Coupled Chemistry-Climate Model Simulations, *Am. Meteor. Soc.*, 905–921, <https://doi.org/10.1175/JAS3866.1>, 2007.
- Boville, B. A., Kiehl, J. T., Rasch, P. J., and Bryan, F. O.: Improvements to the NCAR CSM-1 for Transient Climate Simulations, *J. Climate*, 14, 164–179, [https://doi.org/10.1175/1520-0442\(2001\)014<0164:ITTNCF>2.0.CO;2](https://doi.org/10.1175/1520-0442(2001)014<0164:ITTNCF>2.0.CO;2), 2001.
- Butchart, N., Cionni, I., Eyring, V., Shepherd, T. G., Waugh, D. W., Akiyoshi, H., Austin, J., Brühl, C., Chipperfield, M. P., Cordero, E., Dameris, M., Deckert, R., Dhomse, S., Frith, S. M., Garcia, R. R., Gettelman, A., Giorgetta, M. A., Kinnison, D. E., Li, F., Mancini, E., McLandress, C., Pawson, S., Pitari, G., Plummer, D. A., Rozanov, E., Sassi, F., Scinocca, J. F., Shibata, K., Steil, B., and Tian, W.: Chemistry-Climate Model Simulations of Twenty-First Century Stratospheric Climate and Circulation Changes, *J. Climate*, 23, 5349–5374, <https://doi.org/10.1175/2010JCLI3404.1>, 2010.
- Chiodo, G. and Polvani, L. M.: Reduced Southern Hemispheric circulation response to quadrupled CO₂ due to stratospheric ozone feedback, *Geophys. Res. Lett.*, 44, 465–474, <https://doi.org/10.1002/2016GL071011>, 2017.
- Dee, D. P., Uppala, S. M., Simmons, A. J., Berrisford, P., Poli, P., Kobayashi, S., Andrae, U., Balmaseda, M. A., Balsamo, G., Bauer, P., Bechtold, P., Beljaars, A. C. M., van de Berg, L., Bidlot, J., Bormann, N., Delsol, C., Dragani, R., Fuentes, M., Geer, A. J., Haimberger, L., Healy, S. B., Hersbach, H., Hólm, E. V., Isaksen, I., Kållberg, P., Köhler, M., Matricardi, M., McNally, A. P., Monge-Sanz, B. M., Morcrette, J.-J., Park, B.-K., Peubey, C., de Rosnay, P., Tavolato, C., Thépaut, J.-N., and Vitart, F.: The ERA-Interim reanalysis: configuration and performance of the data assimilation system, *Q. J. Roy. Meteor. Soc.*, 137, 553–597, <https://doi.org/10.1002/qj.828>, 2011.
- Dessler, A. E., Weinstock, E. M., Hints, E. J., Anderson, J. G., Webster, C. R., May, R. D., Elkins, J. W., and Dutton, G. S.: An examination of the total hydrogen budget of the lower stratosphere, *Geophys. Res. Lett.*, 21, 2563–2566, 1994.
- digital dutch: <https://www.digitaldutch.com/atmoscalc/>, (last access: January 2018), 1999.
- ECMWF: IFS DOCUMENTATION – Cy31r1, Part IV: Physical Processes, <https://www.ecmwf.int/sites/default/files/elibrary/2007/9221-part-iv-physical-processes.pdf> (last access: 4 July 2018), 2007.
- Eichinger, R., Jöckel, P., Brinkop, S., Werner, M., and Losow, S.: Simulation of the isotopic composition of stratospheric water vapour – Part 1: Description and evaluation of the EMAC model, *Atmos. Chem. Phys.*, 15, 5537–5555, <https://doi.org/10.5194/acp-15-5537-2015>, 2015.
- Forster, P. M. D. F. and Shine, K. P.: Stratospheric water vapour changes as a possible contributor to observed stratospheric cooling, *Geophys. Res. Lett.*, 26, 3309–3312, <https://doi.org/10.1029/1999GL010487>, 1999.
- Fueglistaler, S. and Haynes, P. H.: Control of interannual and longer-term variability of stratospheric water vapor, *J. Geophys. Res.*, 110, D24108, <https://doi.org/10.1029/2005JD006019>, 2005.
- German Aerospace Center (DLR): The highly structured Modular Earth Submodel System (MESSy), available at: <http://www.messy-interface.org>, last access: 6 July 2018.
- Gromov, S., Jöckel, P., Sander, R., and Brenninkmeijer, C. A. M.: A kinetic chemistry tagging technique and its application to modelling the stable isotopic composition of atmospheric trace gases, *Geosci. Model Dev.*, 3, 337–364, <https://doi.org/10.5194/gmd-3-337-2010>, 2010.
- Hurst, D., Dutton, G., Romashkin, P., Wamsley, P., Moore, F., Elkins, J., Hints, E., Weinstock, E., Herman, R., Moyer, E., Scott, D., May, R., and Webster, C.: Closure of the total hydrogen budget of the northern extratropical lower stratosphere, *J. Geophys. Res.-Atmos.*, 104, 8191–8200, 1999.

- IPCC: Climate Change 2013: The Physical Science Basis. Contribution of Working Group I to the Fifth Assessment Report of the Intergovernmental Panel on Climate Change, Cambridge University Press, Cambridge, United Kingdom and New York, NY, USA, <https://doi.org/10.1017/CBO9781107415324>, available at: www.climatechange2013.org (last access: 4 July 2018), 2013.
- Jöckel, P., Kerkweg, A., Pozzer, A., Sander, R., Tost, H., Riede, H., Baumgaertner, A., Gromov, S., and Kern, B.: Development cycle 2 of the Modular Earth Submodel System MESSy2, *Geosci. Model Dev.*, 3, 717–752, <https://doi.org/10.5194/gmd-3-717-2010>, 2010.
- Jöckel, P., Tost, H., Pozzer, A., Kunze, M., Kirner, O., Brenninkmeijer, C. A. M., Brinkop, S., Cai, D. S., Dyroff, C., Eckstein, J., Frank, F., Garny, H., Gottschaldt, K.-D., Graf, P., Grewe, V., Kerkweg, A., Kern, B., Matthes, S., Mertens, M., Meul, S., Neu-maier, M., Nützel, M., Oberländer-Hayn, S., Ruhnke, R., Runde, T., Sander, R., Scharffe, D., and Zahn, A.: Earth System Chemistry integrated Modelling (ESCI-Mo) with the Modular Earth Submodel System (MESSy) version 2.51, *Geosci. Model Dev.*, 9, 1153–1200, <https://doi.org/10.5194/gmd-9-1153-2016>, 2016.
- Johnston, H. and Kinnison, D.: Methane photooxidation in the atmosphere: Contrast between two methods of analysis, *J. Geophys. Res.*, 103, 21967–21984, 1998.
- le Texier, H., Solomon, S., and Garcia, R. R.: The role of molecular hydrogen and methane oxidation in the water vapour budget of the stratosphere, *Q. J. Roy. Meteor. Soc.*, 114, 281–295, <https://doi.org/10.1002/qj.49711448002>, 1988.
- Lehmann, R.: An Algorithm for the Determination of All Significant Pathways in Chemical Reaction Systems, *J. Atmos. Chem.*, 47, 45–78, <https://doi.org/10.1023/B:JOCH.0000012284.28801.b1>, 2004.
- MacKenzie, I. A. and Harwood, R. S.: Middle-atmospheric response to a future increase in humidity arising from increased methane abundance, *J. Geophys. Res.*, 109, D02107, <https://doi.org/10.1029/2003JD003590>, 2004.
- Maycock, A. C., Joshi, J. M., Shine, K. P., Davis, S. M., and Rosenlof, K. H.: The potential impact of changes in lower stratospheric water vapour on stratospheric temperatures over the past 30 years, *Q. J. Roy. Meteor. Soc.*, 26, 2176–2185, <https://doi.org/10.1002/qj.2287>, 2014.
- McCormack, J. P., Hoppel, K. W., and Siskind, D. E.: Parameterization of middle atmospheric water vapor photochemistry for high-altitude NWP and data assimilation, *Atmos. Chem. Phys.*, 8, 7519–7532, <https://doi.org/10.5194/acp-8-7519-2008>, 2008.
- MESSy Consortium: <http://www.messy-interface.org> (last access: 6 July 2018)
- Monge-Sanz, B. M., Chipperfield, M. P., Untch, A., Morcrette, J.-J., Rap, A., and Simmons, A. J.: On the uses of a new linear scheme for stratospheric methane in global models: water source, transport tracer and radiative forcing, *Atmos. Chem. Phys.*, 13, 9641–9660, <https://doi.org/10.5194/acp-13-9641-2013>, 2013.
- Mote, P.: The annual cycle of stratospheric water vapor in a general circulation model, *J. Geophys. Res.*, 100, 7363–7379, <https://doi.org/10.1029/94JD03301>, 1995.
- Myhre, G., Nilsen, J. S., Gulstad, L., Shine, K. P., Rognerud, B., and Isaksen, I. S. A.: Radiative forcing due to stratospheric water vapour from CH₄ oxidation, *Geophys. Res. Lett.*, 34, L01807, <https://doi.org/10.1029/2006GL027472>, 2007.
- NOAA/NASA: US Standard Atmosphere 1976 (NASA-TM-X-74335), National Oceanic and Atmospheric Administration/National Aeronautics and Space Administration, United States Air Force, US Government Printing Office, Washington, DC, <https://docs.google.com/file/d/0B2UKsBO-ZMVgWG9mWEJGMIFacDQ/edit> (last access 6 July 2018), 1976.
- Oman, L., Waugh, D. W., Pawson, S., Stolarski, R. S., and Nielsen, J. E.: Understanding the Changes of Stratospheric Water Vapor in Coupled Chemistry–Climate Model Simulations, *J. Atmos. Sci.*, 65, 3278–3291, <https://doi.org/10.1175/2008JAS2696.1>, 2008.
- Rahn, T., Eiler, J. M., Boering, K. A., Wennberg, P. O., McCarthy, M. C., Tyler, S., Schauffler, S., Donnelly, S., and Atlas, E.: Extreme deuterium enrichment in stratospheric hydrogen and the global atmospheric budget of H₂, *Nature*, 424, 918–921, <https://doi.org/10.1038/nature01917>, 2003.
- Revell, L., Stenke, A., Rozanov, E., Ball, W., Lossow, S., and Peter, T.: The role of methane in projections of 21st century stratospheric water vapour, *Atmos. Chem. Phys.*, 16, 13067–13080, <https://doi.org/10.5194/acp-16-13067-2016>, 2016.
- Revell, L. E., Bodeker, G. E., Huck, P. E., Williamson, B. E., and Rozanov, E.: The sensitivity of stratospheric ozone changes through the 21st century to N₂O and CH₄, *Atmos. Chem. Phys.*, 12, 11309–11317, <https://doi.org/10.5194/acp-12-11309-2012>, 2012.
- Roeckner, E., Brokopf, R., Esch, M., Giorgetta, M., Hagemann, S., Kornblüeh, L., Manzini, E., Schlese, U., and Schulzweida, U.: Sensitivity of Simulated Climate to Horizontal and Vertical Resolution in the ECHAM5 Atmosphere Model, *Am. Meteorol. Soc.*, 19, 3771–3791, 2006.
- Rohs, S., Schiller, C., Riese, M., Engel, A., Schmidt, U., Wetter, T., Levin, I., Nakazawa, T., and Aoki, S.: Long-term changes of methane and hydrogen in the stratosphere in the period 1978–2003 and their impact on the abundance of stratospheric water vapor, *J. Geophys. Res.-Atmos.*, 111, 1–12, <https://doi.org/10.1029/2005JD006877>, 2006.
- Sander, R., Kerkweg, A., Jöckel, P., and Lelieveld, J.: Technical note: The new comprehensive atmospheric chemistry module MECCA, *Atmos. Chem. Phys.*, 5, 445–450, <https://doi.org/10.5194/acp-5-445-2005>, 2005.
- Sander, R., Baumgaertner, A., Gromov, S., Harder, H., Jöckel, P., Kerkweg, A., Kubistin, D., Regelin, E., Riede, H., Sandu, A., Taraborrelli, D., Tost, H., and Xie, Z.-Q.: The atmospheric chemistry box model CAABA/MECCA-3.0, *Geosci. Model Dev.*, 4, 373–380, <https://doi.org/10.5194/gmd-4-373-2011>, 2011.
- Sander, R., Jöckel, P., Kirner, O., Kunert, A. T., Landgraf, J., and Pozzer, A.: The photolysis module JVAL-14, compatible with the MESSy standard, and the JVal PreProcessor (JVPP), *Geosci. Model Dev.*, 7, 2653–2662, <https://doi.org/10.5194/gmd-7-2653-2014>, 2014.
- Sander, S. P., Abbatt, J., Barker, J. R., Burkholder, J. B., Friedl, R. R., Golden, D. M., Huie, R. E., Kolb, C. E., Kurylo, M. J., Moortgat, G. K., Orkin, V. L., and Wine, P. H.: Chemical Kinetics and Photochemical Data for Use in Atmospheric Studies, Evaluation No. 17, JPL Publication 10-6, Jet Propulsion Laboratory, <https://doi.org/10.1002/kin.550171010>, available at: <http://jpldataeval.jpl.nasa.gov/> (last access: 4 July 2018), 2011.
- Solomon, S., Rosenlof, K. H., Portmann, R. W., Daniel, J. S., Davis, S. M., Sanford, T. J., and Plattner, G.-K.: Contri-

- butions of Stratospheric Water Vapor to Decadal Changes in the Rate of Global Warming, *Science*, 327, 1219–1223, <https://doi.org/10.1126/science.1182488>, 2010.
- Stenke, A. and Grewe, V.: Simulation of stratospheric water vapor trends: impact on stratospheric ozone chemistry, *Atmos. Chem. Phys.*, 5, 1257–1272, <https://doi.org/10.5194/acp-5-1257-2005>, 2005.
- Stowasser, M., Oelhaf, H., Wetzell, G., Friedl-Vallon, F., Maucher, G., Seefeldner, M., Trieschmann, O., v. Clarmann, T., and Fischer, H.: Simultaneous measurements of HDO, H₂O, and CH₄ with MIPAS-B: Hydrogen budget and indication of dehydration inside the polar vortex, *J. Geophys. Res.*, 104, 19213–19225, 1999.
- UCAR/NCAR/CISL/TDD: The NCAR Command Language (Version 6.4.0) [Software], Boulder, Colorado: UCAR/NCAR/CISL/TDD, <https://doi.org/10.5065/D6WD3XH5>, 2017.
- Wrotny, J. E., Nedoluha, G. E., Boone, C., Stiller, G. P., and McCormack, J. P.: Total hydrogen budget of the equatorial upper stratosphere, *J. Geophys. Res.-Atmos.*, 115, D04302, <https://doi.org/10.1029/2009JD012135>, 2010.